February 1998
Melbourne Australia

PROCEEDINGS OF THE 2ND INTERNATIONAL CONFERENCE ON BIOELECTROMAGNETISM

15 - 18 February 1998
Melbourne, AUSTRALIA

Edited by:
Brian Lithgow — Program Co Chairman
Irena Cosic — Conference Chairman

Organised by :

Monash University
- Bioelectronics Group
  Department of Electrical & Computer Systems Engineering
- Office of Continuing Education

In cooperation with :
The International Society for Bioelectromagnetism
Engineering in Medicine and Biology - IEEE
International Federation for Medical & Biological Engineering
Australian College of Physical Scientists & Engineers in Medicine

SPONSORED BY

Dick Wicks
Magnetic Pain Relief Products

Foundation for
East West Medicine - Taiwan

PREFACE

The 2nd International Conference on Bioelectromagnetism (2nd ICBEM) brings together biomedical engineers and scientists from around the world to present and discuss the latest advances in the areas of field measurements, electric and magnetic stimulation, signal and image analysis, electromagnetic field effects, electric and magnetic impedance, electromagnetic properties of alternative medicines and biomolecular electronics. The 1st International Conference on Bioelectromagnetism was organised together with the 10th Nordic-Baltic Conference on Biomedical Engineering, in Tampere, Finland, and it was a great success. This time, in Melbourne, the International Conference on Bioelectromagnetism stands alone, showing that bioelectromagnetism has become a separate discipline attracting substantial research. The Proceedings of the 2nd International Conference on Bioelectromagnetism documents the efforts of those engineers and scientists. These efforts describe the application of modern scientific and engineering tools to the solution of medical diagnosis and treatment problems.

Irena Cosic
Conference Chair

The Proceedings have been published under the IEEE book broker program and are catalogued by an ISBN number and are available for purchase through IEEE. All papers included in the Proceedings of the 2nd ICBEM have been reviewed and accepted by the Program Committee. Based on the paper types submitted these Proceedings are subdivided into twelve tracks, namely, fields, signal and image analysis, tissues, instruments, molecules, impedance, electromagnetic interactions, stimulation, cardiography, ultrasound and electric field, power lines and electromagnetic interactions and acupuncture.

The hard work and close cooperation of a large number of people have contributed to the success of this meeting. Our colleagues on the organising, international advisory and scientific committees have given generously of their time over the past two years.

There is a considerable international presence at this conference, highlighting the need for further such meetings and highlighting the importance of understanding the bioelectric and biomagnetic phenomena which form the basis of many biological processes from the cellular to the organism level. Finally, we would like to thank the authors and their colleagues for their valuable contributions to these Proceedings

Brian Lithgow
Program Co-chair

Irena Cosic
Conference Chair

Brian Lithgow
Program Co-chair

RBS54/09

INTERNATIONAL ADVISORY COMMITTEE

Jaakko Malmivuo (Finland)
Metin Akay (USA)
Tatsuo Togawa (Japan)
Robert Plonsey (USA)
Rajko Tomovic (Yugoslavia)
Tina Karu (Russia)
Yuan Ting Zang (Hong Kong)
Fumihio Kajiya (Japan)
Susan Blanchard (USA)
Julia Tsuei (Taiwan)
Shoogo Ueno (Japan)
Hiie Hinrikus (Estonia)
Wilson Greatbatch (USA)
Pak Chung Ching (Hong Kong)

SCIENTIFIC COMMITTEE

Irena Cosic (Australia) **Chairman**
Brian Lithgow (Australia) **Co-chairman**
Jaakko Malmivuo (Finland) **Co-chairman**
Metin Akay (USA) **Co-chairman**
Andy Daubenspeck (USA)
Bhavin Mehta (USA)
Jacques Duchene (France)
Hartmut Dickhaus (Germany)
Yuan Ting Zang (Hong Kong)
Anthony Rees (UK)
Ken Joyner (Australia)
Dale Murphy (Australia)
David Kilpatrick (Australia)
Robert Shepherd (Australia)
Janie Fouke (USA)
Keith Paulsen (USA)
Patrick Celka (Switzerland)
Janet Rutledge (USA)
Hidetoshi Matsuki (Japan)
Malvin Teich (USA)
Makoto Yoshizawa (Japan)
Daming Wei (Japan)
Richard Jones (NZ)
Robert Barnett (Australia)
Stig Ollmar (Sweden)
Lars Korsnes (Norway)
Leonid Titomir (Russia)
Tina Karu (Russia)
Richard Potember (USA)
Shunsuke Sato (Japan)
Kazuo Yana (Japan)
Dan Stroud (Australia)

ORGANISING COMMITTEE

Irena Cosic **Chairman**
Brian Lithgow **Co-chairman**
Jaakko Malmivuo **Co-chairman**
Metin Akay **Co-chairman**

The Bioelectronics Group

Marc Cohen
Brett Heath
Steven Birch
Eliada Lazoura
John (Qiang) Fang
Maia Rozenfeld
Elena Pirogova
Peter Ciblis

CONFERENCE MANAGERS

Irene Thavarajah & Maureen Kemp
Office of Continuing Education
Monash University

TABLE OF CONTENTS

TABLE OF CONTENTS

TISSUES

STATE OF THE ART SPEAKER

INSTRUMENTS

SIGNAL & IMAGE ANALYSIS

MOLECULES

IMPEDANCE

TABLE OF CONTENTS

ELECTROMAGNETIC INTERACTIONS

MOLECULES

IMPEDANCE

ELECTROMAGNETIC INTERACTIONS

STIMULATION

TABLE OF CONTENTS

STATE OF THE ART SPEAKER

CARDIOGRAPHY

ULTRASOUND & ELECTRIC FIELD

STIMULATION

CARDIOGRAPHY

TABLE OF CONTENTS

POWER LINES & ELECTROMAGNETIC INTERACTIONS

ACUPUNCTURE

STATE OF THE ART SPEAKER

CARDIOGRAPHY

ELECTROMAGNETIC INTERACTIONS

History, Present Status and Future of Bioelectromagnetism

Jaakko Malmivuo, President ISBEM
Ragnar Granit Institute, Tampere University of Technology
P.O. Box 692, FIN-33101 Tampere, Finland
http://www.cc.tut.fi/~malmivuo/BEM/bem.htm

Abstract: The discipline of bioelectromagnetism is 6000 years old. Bioelectric methods have developed to very important diagnostic and therapeutic methods in the modern medicine. Large investments are made to develop also the biomagnetic applications for medical use. Their future is, however, still unclear.

HISTORY

Bioelectromagnetism is one of the oldest disciplines. The first written document dates back to 4000 B.C. During its early phase it was similarly scientific and mythic as medicine. The first comprehensive presentation, which could be considered as scientific, was written 1600 by William Gilbert entitled "De Magnete". Interesting is, that the name of this book was not "De Electricite"

The invention of the connection between electricity and magnetism by H.C. Örstedt in 1819 was revolutionary in the development of our discipline. It made possible to develop the galvanometer and especially the astatic galvanometer by Leopold Nobili in 1825, the instrument for measuring the bioelectric phenomenon. Actually what was measured was the magnetic field induced directly by the (unamplified) bioelectric current flowing in a coil connected directly to the preparate. The source of this magnetic field, however, was not the vortex source but the flux source. Benjamin Franklin invented in 1831 the induction coil making continuous electric stimulation possible.

Measurement of the flux source has developed to a very powerful clinical diagnostic method. Willem Einthoven laid the ground for applying this technique to the heart and Hans Berger to the brain.

Improved instrumentation like vacuum tube and later semiconductor amplifiers as well as display systems like the oscilloscope made the measurement of the flux source a practical, cheap and non-invasive clinical method. Like in every other field of life, the very fast developed data processing facilities have further improved the diagnostic performance of bioelectric methods.

BIOMAGNETISM

The first measurement of one component of the vortex source of the heart was made by Richard McFee in 1963. He also established the theory of biomagnetic measurements. It was based on the lead field theory which he developed on the basis of the reciprocity theorem of Helmholtz.

For a long time there existed the dilemma: Why the biomagnetic signal was not fully independent of the bioelectric one though it was thought that on the basis of the Helmholtz' Theorem they should have been. If that had been the case, the biomagnetic recordings had been a new revolutionary, non-invasive measurement technique.

Jaakko Malmivuo developed the practical method for recording all the three components of the vortex source. He also gave an explanation for applying the Helmholtz' theorem to the independence of bioelectric and biomagnetic signals.

PRESENT STATUS

At present, the measurement of the flux source with bioelectric methods has a very strong position as a clinical diagnostic method. Similarly, electric stimulation, especially the pacemaker, is a standard therapeutic method.

In developing the measurement of the vortex source, the investments to biomagnetism, especially in MEG, are massive. There exist some 40 large scale MEG instrumentations and a large number of other smaller ones in the world. In MCG the research is not so active.

Despite of the large investments to MEG, there does not exist even a single publication fulfilling the criteria of a clinical study comparing the relative merits of EEG and MEG as a clinical tool! This is a serious deficiency of the technique because it cannot be accepted to clinical practice before such studies are successfully made.

In MCG there exist several studies where, by mapping the magnetic field in front of the thorax, it is mainly measured the flux source instead of the vortex source. Therefore, and because the usually small patient materials, these studies have not succeeded to convince of the superiority of MCG over ECG. There, however, exist one study with clinically sufficient patient material, where it was measured both the vortex and the flux sources with the MCG and the ECG, respectively. When combining these signals, it was succeeded to decrease the number of incorrectly diagnosed patients to one half.

FUTURE

Without doubt the existing modelling methods and computer facilities will further develop the value of the bioelectric methods measuring the flux source. The future of these techniques is, without doubt, bright.

The future of biomagnetism is a question mark. There is evidence that the MCG is rather successful. Is it successful enough to support applying the technique in large number is not fully clear yet. Some special applications like fetal MCG, where the detection of the vortex source itself is not important, but important is that the sensitivity distribution of this measurement makes it possible for the technique to "penetrate" through the fat layer of the fetus, may make MCG an important clinical tool.

There is no doubt, that understanding the fundamental principles of bioelectromagnetism, the Maxwell's Equations and the Principle of Reciprocity, which tie all the subdivisions of the discipline tightly together, will facilitate the development of this important discipline.

Is Accurate Recording of the Surface Laplacian Feasible?

David B. Geselowitz, Jason Ferrara
Bioengineering Program, Pennsylvania State University
232 Hallowell Building., University Park, PA 16801

Abstract: Experimental and model studies were performed to measure the surface Laplacian using a rectangular finite difference approximation. The experimental approach used 10 normal subjects with two sites on the torso. Electrode spacing was 2 cm. The surface Laplacian is theoretically independent of rotation of the electrode array. The data showed considerable variation with rotation. Model studies employed a realistic 23 dipole source. A spherical volume conductor showed invariance with rotation, as anticipated theoretically. A realistic torso, however, showed variation with rotation, although a not as severe as that measured. The average signal to noise ratio was 3.3 and 2.5 at the two sites. These results raise serious questions about the practical ability to measure the surface Laplacian on the torso.

INTRODUCTION

The use of the surface Laplacian, **L**, for skin potentials was first proposed by Hjort [1] for studying the electroencephalogram and later by He et al [2] for the electrocardiogram. One rationale is that **L** will give different and perhaps more localized information concerning the sources which give rise to the surface potential distribution, V. It has also been proposed that use of **L** rather than the potential will enhance the solution of the inverse problem.

On a flat surface $\mathbf{L} = \partial^2 V/\partial x^2 + \partial^2 V/\partial y^2$ where x,y are the Cartesian coordinates of a point on the surface. As an approximation,

$$L(x,y) \approx \frac{V(x+d,y)+V(x-d,y)+V(x,y+d)+V(x,y-d)-4V(x,y)}{d^2}$$

which can be measured by an array of 5 electrodes where d is the distance from the center electrode to each of the other 4 electrodes. This approximation is valid for a sphere provided that d is interpreted as the distance along the surface of the sphere.

The surface Laplacian is invariant with respect to a rotation of axes. Therefore the measurement should not change significantly with a rotation. In practice, a variation might be observed because of the curvature of the surface and the finite separation, d. Such variation would indicate inappropriateness of the flat surface approximation.

METHOD

Surface Laplacian recordings were obtained using a five electrode array. Recordings were taken from 10 subjects, using a grid spacing of 2cm. The subjects were normal males in the age range of 20-32 years. Two locations were used, one to the left of the center of the chest and one near the left shoulder. An electrode template was cut out of a thin sheet of flexible plastic. Self adhesive Ag/AgCl electrodes (Graphic Controls model 5500 Q-Trace Gold) were placed over each of the five holes on the template to form the electrode array.

For each recording location, two recordings were taken, one with the y axis of the electrode grid oriented in the head to foot direction, and one with it rotated 45°. Approximately one minute of data was recorded for each recording location and orientation. Each data set consisted of four difference voltages together with their average, which is proportional to the surface Laplacian.

Four differential amplifiers and a multi-channel analog to digital converter (BIOPAC MP100A) connected to a computer were used. The center electrode was connected to the negative input of each amplifier. Each of the peripheral electrodes was connected to the positive input of an amplifier. The outputs of the four amplifiers were averaged using a resistor network. This analog average agreed with a digital one obtained subsequently. The amplifiers had a low frequency cutoff of 0.05 Hz, and a high frequency cutoff of 1 KHz. The individual potentials and their average were recorded. The MP100A had a resolution of 16 bits, a range of ±10 volts, and a sampling rate of 3237.29 Hz.

In several instances severe problems with 60 Hz noise were encountered. To remove the noise, digital filtering was performed on the signals after they had been recorded. The recordings were first passed through a 60 Hz notch filter, and then though a 100 Hz lowpass filter. The recordings which were noise free were also run though this series of filters, and then compared to the unfiltered signal to insure that the filters were not causing any distortion of the signal.

The recordings were analyzed for noise content. A signal averaging technique was used to separate the signal from the noise. A window just enclosing QRS was selected from a lead with a prominent QRS complex, and the signal averaged over the order of 30 beats. The RMS value of the averaged QRS complexes was calculated for the individual difference leads as well as for **L**. The average signal was then subtracted from each signal to provide an estimate of the noise. The RMS of the noise was then calculated.

RESULTS

The average voltage in the difference leads was 83 ± 42 μV for the chest region and 44 ± 33 μV for the shoulder

region. The RMS noise level in the individual difference leads was 16 ± 11 μV for both regions. The average signal to noise ratio of the surface Laplacian was 3.25 ± 1.26 for the chest recordings and 2.46 ± 1.97 for the shoulder recordings. Three of the 20 shoulder recordings exhibited signal to noise ratios of less than one.

For the chest recordings on the 10 subjects, a comparison of **L** recorded with the two electrode orientations showed that 4 waveforms were similar and 5 waveforms were grossly different. For the shoulder recordings with the two orientations, 4 were similar and 5 were grossly different. There was no consistency among subjects with regard to similarity of chest and shoulder determinations of the surface Laplacian. There was considerable variation in the amplitudes and waveshapes of **L** recorded at the chest and shoulder locations among the 10 subjects.

MODEL STUDIES

To put the experimental studies in perspective, model studies were performed using a realistic cardiac source in a homogeneous torso. Two volume conductors were considered, a sphere and a realistic torso. The cardiac source was a 23 dipole model of cardiac excitation and recovery developed by Miller and Geselowitz for the normal heart [3].

Calculations for the sphere used an analytic expression for the potential [4]. The realistic torso was described by 392 triangles. The region where the surface Laplacian was to be determined was subdivided to give a total of between 1745 and 3511 triangles.

The surface Laplacian was calculated at two sites for both the sphere and realistic torso. These sites corresponded to those used experimentally. In all cases the electrode separation, d, was varied from 1 to 4 cm in steps of 1 cm. The angle of rotation of the electrode array was varied in steps of 9°.

For the sphere the value of **L** remained constant as d varied from 1 to 4 cm. The total change was less than 2%. Furthermore as the angle varied, **L** remained constant. For the realistic torso, on the other hand, the peak value of **L** varied from 238 to 121 $\mu V/cm^2$ as spacing increased from 1 to 4 cm in the chest region, and from 8.5 to 4.0 $\mu V/cm^2$ in the shoulder region.

In contrast to the sphere, **L** for the realistic torso varied with angle. For the chest site for d = 2 cm, the maximum increased by 4.6% and the minimum increased by 11.5% at 45° while for the shoulder the change was 23.3% and 7.7%. Greater discrepancies were observed at some intermediate rotations.

DISCUSSION

Aside from theoretical concerns, there are two practical issues regarding the utility of using the surface Laplacian. One is the signal to noise ratio. The other is the ability to record it on the curved surface of the torso. The present study investigated these aspects with a modest experimental study together with model studies.

The algorithm for **L** involves small difference signals, and may be expected to exhibit poor signal to noise ratio. The experimental data indicated that there are potentially severe signal to noise problems. A low signal to noise ratio would make inverse calculations difficult, and would hamper interpretation of the signals themselves.

One test of the accuracy of the rectangular electrode array is whether **L** is invariant with rotation. Our results reveal substantial effects of rotation. On a flat surface **L** has a simple expression. The expression on an arbitrary surface is extremely complex, and involves the local curvature, and would be difficult to implement. All investigators have used the flat surface approximation. To test the effect of curvature we used the simple expression and compared results with the array rotated 45°. For the 2 cm spacing used vast differences were recorded, indicating severe limitations in the ability to record **L** accurately. The model studies tended to confirm the experimental results, although the variation found was not as severe. For a spherical surface there was no effect of rotation of the electrode array as predicted theoretically. On the realistic torso, however, variations of greater than 23% were obtained in peaks of the biphasic waveform.

The realistic torso model for d = 2 cm gave peak values of **L** of about 150 $\mu V/cm^2$ for the chest and 12 $\mu V/cm^2$ for the shoulder. The experimental results exhibited a great variation, with 7 of the 10 subjects having higher amplitudes in the chest recordings.

The surface Laplacian has also been measured using a ring electrode, again based on a planar surface. The ring electrode suffers from the additional problem that good uniform contact must be obtained with the skin along the entire perimeter.

These results raise serious questions about the practically of measuring **L** on the body surface.

REFERENCES

[1] B. Hjort, "An on-line transformation of EEG scalp potentials into orthogonal source derivations", *Electroenceph. Clin. Neurophysiol.*, 39:526-530, 1975.

[2] B. He, R.J. Cohen, "Body surface Laplacian ECG mapping", *IEEE Transactions on Biomedical Engineering* BME-39: 1179-1191, 1992.

[3] W. T. Miller, III and D. B. Geselowitz, "Simulation studies of the electrocardiogram. I. The normal heart," *Circulation Research*, 43:301-315, 1978.

[4] E. Frank, "Electric potential produced by two point current sources in a homogeneous conducting sphere", J Applied Physics, 23:1225-1228, 1952.

ACKNOWLEDGMENT

This work was supported in part by a grant HL36625 from the National Institutes of Health.

Modeling the Volume Conductor – Double Fourier Series Approximation Versus Spherical Harmonic Expansion

Gerhard Lafer, Paul Wach, Bernhard Tilg
Department of Biophysics, Institute of Biomedical Engineering,
Graz University of Technology, A-8010 Graz, Austria

ABSTRACT: A method for parametric description of boundary surfaces based on combined second order surface and double Fourier series approximation is presented. Gauss transformation is used to determine the best fitting parameters. The method is applied to approximate the conductivity interfaces of volume conductor models needed for solving the bioelectromagnetic forward and inverse problem. The attained quality of fit was compared to that obtained applying the surface harmonic expansion for modeling the volume conductor shape. In that case, the coefficients of expansion are found by nonlinear least-squares fit.

INTRODUCTION

In several areas of medical research, it is necessary to represent accurately morphological characteristics of the human body (e.g. head, torso or internal organs like the brain or heart). Therefore, a three-dimensional (3D) object must be reconstructed from serial cross-sections, either to support the comprehension of the object's structure or to facilitate its automatic manipulation and analysis. Examples include the electrical impedance imaging method [1], or the numerical solution of bioelectric [2] and/or biomagnetic forward and inverse problems [3]. To compute bioelectromagnetic forward and inverse solutions, digitized models of the associated volume conductor are required. It seems that the use of individualized realistically shaped volume conductor models may substantially improve the accuracy of bioelectric and biomagnetic inverse solutions [4]. Hence, an explicit and compact representation/reconstruction of anatomical surfaces would be very advantageous.

We have developed a parametric representation of conductivity interfaces of volume conductor models based on second order surface and double Fourier series approximation [5]. There, an ellipsoid is approximated to the boundary surface of the volume conductor in a first step. Because of the complexity of biological shapes, it is difficult to describe a shape as a simple geometric or other analytic representation. For a more accurate approximation of the corresponding boundary surfaces a subsequent double Fourier series expansion is applied. In another approach the surface harmonic expansion is used to represent boundaries between regions of different conductivity [6]. Both methods were applied to represent the surface of a subject's head and torso. Finally, the quality of approximation attained using surface harmonic expansion and combined ellipsoid double Fourier series approximation was compared.

METHOD

For the coefficient estimation of a parametric representation of three-dimensional closed surfaces a set of measurement points lying on that specific surface is required. The measured nodes of a boundary surface can be extracted from magnetic resonance imaging (MRI) cross-sections. For a given set N_p of measured surface coordinates ${}^p\mathbf{x}_i = ({}^px_i, {}^py_i, {}^pz_i)^\mathbf{T}$ a matrix $\mathbf{M} \in \mathbb{R}^{N_p \times 9}$ is defined so that the i-th row $\mathbf{m}_i$ is

$$\mathbf{m}_i = ({}^px_i^2, {}^py_i^2, {}^pz_i^2, 2\,{}^px_i, 2\,{}^py_i, 2\,{}^pz_i, {}^px_i, {}^py_i, {}^pz_i) \quad (1)$$

Quadratic surface approximations can be applied to coarsely describe boundary surfaces in the three-dimensional space. The general form of a second order surface can be expressed by the following general second-degree equation

$$\mathbf{x}^\mathbf{T}\mathbf{A}\mathbf{x} + \mathbf{B}^\mathbf{T}\mathbf{x} + c = 0, \quad (2)$$

where $\mathbf{A} \in \mathbb{R}^{3\times3}$ is a symmetric matrix with elements $a_{kl} = a_{lk}$, $\mathbf{B} \in \mathbb{R}^{3\times1}$ is a column matrix with elements b_l, and $\mathbf{x} \in \mathbb{R}^3$ is the coordinate vector containing the three Cartesian components. In the following the constant c is assumed to be -1. Eq. (2) can be reduced so that the centre $\mathbf{x_0}$ of the ellipsoid and the origin of the coordinate system coincide:

$$\mathbf{u}^\mathbf{T}\bar{\mathbf{A}}\mathbf{u} - 1 = 0 \quad (3)$$

with $\bar{\mathbf{A}} \in \mathbb{R}^{3\times3}$ defined by $\bar{\mathbf{A}} = 4\left(\mathbf{B}^\mathbf{T}\mathbf{A}^{-1}\mathbf{B} + 4\right)^{-1}\mathbf{A}$. The centre $\mathbf{x_0}$ of the ellipsoid may be obtained by $\mathbf{x_0} = -0.5\mathbf{A}^{-1}\mathbf{B}$. One technique for finding the coefficients a_{kl} in the matrix $\mathbf{A}$ and b_l in $\mathbf{B}$ is to solve the following linear model applying the Gauss transformation

$$\mathbf{M}^\mathbf{T}\mathbf{M}\,\mathbf{c} = \mathbf{M}^\mathbf{T}\mathbf{e} \quad (4)$$

with $\mathbf{c} \in \mathbb{R}^9$, $\mathbf{c} = (a_{11}, a_{22}, a_{33}, a_{12}, a_{13}, a_{23}, b_1, b_2, b_3)^\mathbf{T}$, and $\mathbf{e} \in \mathbb{R}^{N_p}$, $\mathbf{e} = (1, 1, 1, \ldots, 1)^\mathbf{T}$. $\mathbf{M}$ is the measurement matrix defined in (1). For further computations it is advantageous to transform the considered geometry to the spherical polar coordinate system $\boldsymbol{\xi}_\mathbf{s}$

$$\boldsymbol{\xi}_\mathbf{s} = \boldsymbol{\Lambda}^{\frac{1}{2}}\mathbf{T}^{-1}\mathbf{u} \quad (5)$$

where $\boldsymbol{\Lambda}$ is a diagonal matrix defined by $\boldsymbol{\Lambda} = diag\left(\frac{1}{a^2}, \frac{1}{b^2}, \frac{1}{c^2}\right)$ with the eigenvalues of $\bar{\mathbf{A}}$ as diagonal elements, and $\mathbf{T} = (\mathbf{v_1}, \mathbf{v_2}, \mathbf{v_3})$ is an orthogonal transformation matrix, where $\mathbf{v_1}$, $\mathbf{v_2}$, and $\mathbf{v_3}$ are the eigenvectors of $\bar{\mathbf{A}}$.

Often a more accurate reconstruction of the corresponding boundary surface is necessary for reasonable

results in further numerical computations. One possibility to approximate the geometry is applying a subsequent trigonometric series expansion. Therefore, an affine transformation from the ellipsoidal space to the spherical space is performed (5). A two-dimensional periodic function $r_s(\theta,\phi)$ that is even in θ, and that has periods L, and B can be developed in the following double Fourier series [5]

$$r_s(\theta,\phi) = \sum_{n=0}^{\infty}\sum_{m=0}^{\infty}\Big(A_{nm}\cos\left(\tfrac{2\pi}{L}n\theta\right)\cos\left(\tfrac{2\pi}{B}m\phi\right) + B_{nm}\cos\left(\tfrac{2\pi}{L}n\theta\right)\sin\left(\tfrac{2\pi}{B}m\phi\right)\Big) \quad (6)$$

with A_{nm}, and B_{nm} the associated Fourier coefficients. In practice one has to work with a truncated series, where the order N, and M depends on the desired accuracy and the speed of convergence of the series with the particular function considered. The best fitting parameters are found by solving the set of normal equations

$$\mathbf{W^T W\ C = W^T\ R} \quad (7)$$

where $\mathbf{C} \in \mathbb{R}^{\mathbf{N_c}}$ is the vector of coefficients A_{nm}, and B_{nm}, and $\mathbf{R}$ is a vector of the norms $R_i = \|^p\boldsymbol{\xi}_{\mathbf{s}_i}\|$ of the measured points in the spherical space. The design matrix $\mathbf{W} \in \mathbb{R}^{N_c \times N_p}$ of the fitting problem is constructed from the $N_c = (N+1)*(M+1)+(N+1)*M$ basis functions in equation (6), and from the N_p measurement points.

Another possibility to represent boundaries between regions of different conductivity is applying the surface harmonic expansion [6]. Thus, a closed surface in the three-dimensional space can be described by a vector valued function $\mathbf{x}(\theta,\phi)$ with Cartesian components

$$\mathbf{x}(\theta,\phi) = \mathbf{x}_0 + f(\theta,\phi)\begin{bmatrix}\sin(\theta)\cos(\phi)\\ \sin(\theta)\sin(\phi)\\ \cos\theta\end{bmatrix} \quad (8)$$

where $\mathbf{x}_0$ is the origin of the expansion. $f(\theta,\phi)$ is the distance from the origin to a point on the boundary surface and can be approximated by an absolutely convergent series of surface harmonics truncated at N

$$f(\theta,\phi) = \sum_{n=0}^{N}\Big(a_n P_n(\cos\theta) + \sum_{m=1}^{n}\left(a_{nm}\cos m\phi + b_{nm}\sin m\phi\right)P_n^m(\cos\theta)\Big) \quad (9)$$

with P_n and P_n^m the Legendre, and associated Legendre polynomials, respectively. The origin $\mathbf{x}_0$ of expansion and the series coefficients $\mathbf{a} = (a_n, a_{nm}, b_{nm})$ can be determined by a nonlinear least squares fit that minimizes

$$\chi^2(\mathbf{x}_0,\mathbf{a}) = \sum_{i=1}^{N_p}\left|\,{}^p\mathbf{x}_i - \mathbf{x}\left(\mathbf{x}_0, f(\theta_i,\phi_i,\mathbf{a})\right)\right|^2 \quad (10)$$

RESULTS

To measure the quality of fit the root-mean-square (RMS) error was introduced. Figure 1 represents the RMS errors depending on the order of approximation

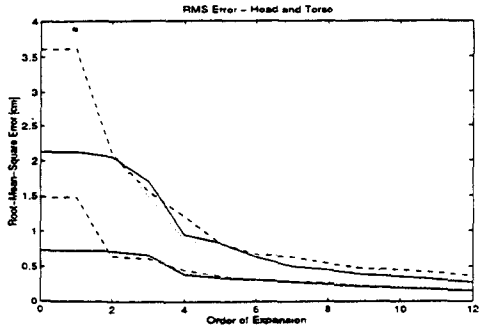

Figure 1. RMS errors depending on the order of approximation in case of the surface of the head (lower curves), and the outer surface of the torso (top curves).

in case of the surface of the head (lower curves), and the outer surface of the torso (top curves). The RMS error applying the combined ellipsoid double Fourier series approximation is depicted with a solid line. Surface harmonic expansions were applied without previous ellipsoid approximation (dashed line), and additional optimal ellipsoid approximation (dotted line).

Both methods, the combined ellipsoid double Fourier series approximation and the surface harmonic expansion provide an accurate and efficient parameterization of boundary shapes, such as the surface of the head or the outer surface of the torso, and can be used together with standard tomographic techniques. The methods can practically applied to the automatic reconstruction of individualized boundary element head and torso models necessary for bioelectromagnetic forward and inverse computations.

REFERENCES

[1] M. Cheney, and D. Isaacson, "Issues in Electrical Impedance Imaging," *IEEE Computational Science & Engineering*, vol. 2(4), pp 53-62, 1995.

[2] B.N. Cuffin, "EEG Localization Accuracy Improvements Using Realistically Shaped Head Models," *IEEE Trans. Biomedical Eng.*, 43(3), pp. 299-303, 1996.

[3] P. Wach, B. Tilg, G. Lafer, and W. Rucker "Magnetic source imaging in the human heart: estimating cardiac electrical sources from simulated and measured MCG data," *Med & Biol Eng & Comput.*, vol. 35, pp. 157 - 166, 1997.

[4] G. Huiskamp, and A. Van Oosterom, "Tailored Versus Realistic Geometry in the Inverse Problem of Electrocardiography," *IEEE Trans. Biomed. Eng.*, vol. 36(8), pp. 827-835, 1989.

[5] P. Wach, G. Lafer, and B. Tilg, "Parametric Approximation of Boundary Surfaces," *1st Austrian Symposium on Noninvasive Functional Source Imaging (NFSI 97), Biomedizinische Technik*, vol. 42 (Ergänzungsband 1), pp. 163-166, 1997.

[6] C. Purcell, T. Mashiko, K. Odaka, and K. Ueno "Describing Head Shape with Surface Harmonic Expansion," *IEEE Trans. Biomed. Eng.*, vol. 38(3), pp. 303-306, 1991.

ACKNOWLEDGEMENT

This work was supported by the Austrian Science Foundation (FWF) with project P11448-MED.

Effect of the skull on scalp potentials

Eskola H, Toivo T, Laarne P, Lahtinen A, Meretoja A-P*, Lang H*, Malmivuo J
Ragnar Granit Institute, Tampere University of Technology
P.O. Box 629, FIN-33101 Tampere, Finland
* University of Turku, Department of Clinical Neurophysiology
FIN-20520 Turku, Finland

ABSTRACT: The skull has low conductivity, which influences especially electroencephalographic (EEG) signals recorded on the scalp, but also the magneto-encephalogram (MEG). Thus the information obtained from these signals can be prominently enhanced, if the effects of the skull can be taken into account. We have used both theoretical and experimental approaches to study these effects to EEG. Our experimental results suggest that the signal transmission from the cortex to the scalp has quite low frequency dependence. The results of theoretical modelling suggest that the overall variation of the skull parameters has a relatively small effect compared to the spatial variations.

1. INTRODUCTION

The quality of the theoretical models for analyzing electroencephalography (EEG) and magnetoencephalography (MEG) is continuously increasing. However, the conductivity data available for these models includes values differing prominently from each other. There exists also individual and local variation both in the geometry and in the conductive properties of tissues. Therefore it is essential to understand the basic effects of various tissues affecting the transmission of the signal from the brain to the scalp.

Theoretical studies on models having various levels of complexity show that the conductivity and thickness of the skull have a marked effect on the non-invasive signals recorded by using either EEG or MEG [1,2,3,4]. The result of these studies is that the poorly conductive bone layer affects both the amplitude and direction of the current arising from the cortical activity. The common result of these studies is that the poorly conductive bone layer affects both the amplitude and direction of the current arising from the cortical activity. Also conductivities and thicknesses of adajcent tissues like scalp and cerebrospinal fluid (CSF) seem to have a marked effect on the signal transmission.

For simplicity practically all theoretical models are derived under quasistationary conditions. Therefore they do not take the effect of the frequency into account. We have used experimental methods for studying the signal transmission as a function of frequency.

2. METHOD

We have used two kind of theoretical models: a fast analytical Laplacian method taking into account the conductivities and thicknesses of the scalp and skull, and a detailed FDM model [5], which in this study is based on the MRI scan of a normal adult subject. The conductivity and thickness parameters were changed in these models within the normal physiological and anatomical range given in the literature.

For displaying the results multimodal 3D reconstructions were used, where the electrical fields were superimposed on the segmented MRI images.

The experimental work was carried out in two kind of studies. The first study consisted of recording the spontaneous EEG of 76 clinically normal children (ages from 3 to 19 years). The other set of experiments was realized by feeding sinusoidal current through a small electrode pair into the cortex of one passive tissue model (a cadaver) and recording of the potentials on the scalp. Digital EEG device (BioLogic) and the standard 10-20 system electrode locations were used in both studies. The data was processed by using both a commercial spectral analysis software and special data analysis procedures designed for this purpose.

3. RESULTS

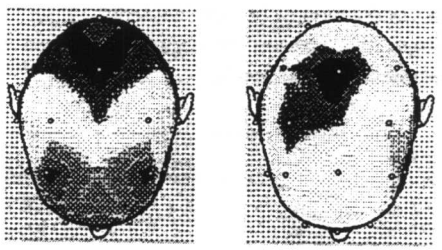

Figure 1. A synthesised symmetrical EEG (left) may be associated with quite asymmetrical intracranial potential distribution (right). The distribution has been calculated by a skull-corrected Laplacian method for a skull which is 50% thinner in left anterior and right posterior areas than on the contralateral side.

Figure 1 shows results from application of our Laplacian method in a case where EEG is symmetrical, but the skull is asymmetrical. Table 1 lists results obtained from the FDM model, where the conductivities of the scalp, skull and CSF have been varied.

Relative change in conductivity	Tissue	Relative change in signal amplitude
10%	Scalp	4%
10%	Skull	4%
10%	CSF	3%
640%	Skull	26%

Table 1. Effect of change in tissue conductivity to the overall signal amplitude of EEG

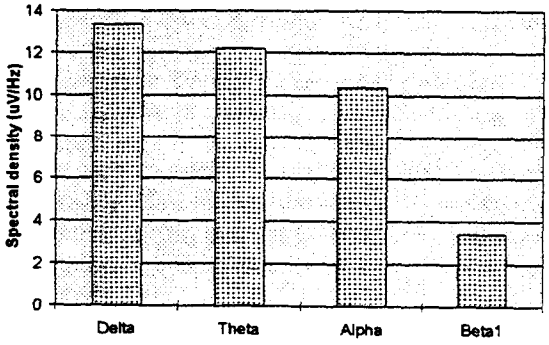

Figure 2. The relative EEG amplitude for EEG rhytms of young subjects corresponding to the frequencies between 1.5 and 20 Hz.

Figure 2 shows the average frequency distribution of EEG for young healthy subjects, while Figure 3 presents the transfer impedance obtained for the experimental tissue model.

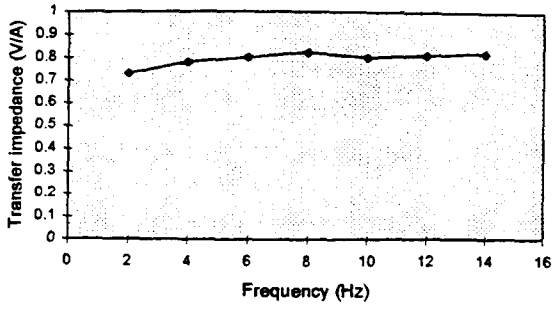

Figure 3. Recorded transfer impedance of the tissues transmitting the signal from the cortex to the scalp.

4. DISCUSSION

The fields in Figure 1 demonstrate qualitatively the clear effect of the thickness variation of the skull to the EEG fields. This particular example illustrates that the subject shows quite asymmetrical electrical brain. function, although the EEG is symmetrical. The same holds in the reciprocal case; an asymmetrical EEG arises on asymmetry of whether the skull or the brain activity.

Table 1 shows that a small 10% deviation in conductivity of one tissue produces about 5% differences to the overall lead fields in the brain. According to the literature the structure and conductivity of the skull may vary considerably. Even more than six times higher conductivity values have been reported, but as can be seen, those affect the lead fields only 26 percents. One conclusion from Fig 1 and Table 1 could be that inter-individual variations in the skull properties are not so important than local changes.

According to Figure 2 the signal amplitude of EEG seems to slightly decrease from low frequencies to the alpha band, which is around 10 Hz. At frequencies higher than 14 Hz the amplitude falls rapidly. This is a well-known feature, generally explained as a *low-pass filtering effect* of the skull. However, this is not in accordance with our experimental results in Figure 3. The skull and other tissues affecting the signal transmission seem not to be responsible for the decrease of the EEG signal with increasing frequency, they may even damp the lowest frequencies. This result also suggests that omitting the effect of frequency in conductivity models does not produce significant errors.

5. REFERENCES

[1] S. Rush and D. Driscoll, "EEG Electrode sensitivity - an application of reciprocity," *IEEE Trans Biomed Eng*, pp. 15-22, 1969.

[2] Y. Eshel, S. Witman, M. Rosenfeld and S Abboud, "Correlation between skull thickness asymmetry and scalp potential estimated by a numerical model of the head," *IEEE Trans Biomed Eng*, pp. 242-249, 1995.

[3] M. Lehtinen, K. Forsman, J. Malmivuo and H. Eskola, "Effects of the skull and scalp thickness on EEG," *Med Biol Eng Comput*, vol. 34, Suppl 1, Part 2, pp. 263-264, 1996.

[4] J. Malmivuo, V. Suihko and H. Eskola, "Sensitivity distributions of EEG and MEG measurements," *IEEE Trans Biomed Eng*, vol. 44, pp. 196-208, 1997.

[5] P. Laarne, H. Eskola, J. Hyttinen, V. Suihko and J. Malmivuo, "Validation of a detailed computer model for the electric fields in the brain," *J Med Engin & Technol*, vol 19(2-3), pp. 84-87, 1995.

Spectral Analysis of Bioelectric Signals by Adapted Wavelet Transforms

Urban Wiklund* and Metin Akay**
*Departments of Biomed. Eng. and Clinical Physiology, University Hospital, S-901 85 Umeå, Sweden
**Thayer School of Eng., Darthmouth College, 8000 Cummings Hall, Hanover, NH 03755-8000 USA

ABSTRACT: *In this study we use the adapted wavelet transform methods (wavelet and cosine packets) for spectral analysis of bioelectric signals. These methods have recently been introduced for analysis of non-stationary signals. Using recordings of the heart rate variability in twenty healthy subjects, the estimated power in different frequency bands is compared to results based on the classical methods: fast Fourier transform and autoregressive modelling.*

Results: Cosine packets gave similar results as the classical methods, and may be preferred to characterise the rhythmic components in the recorded signals. On the other hand, the non-stationary fluctuations, i.e., the "trend", was efficiently decomposed using the wavelet transform method.

1. INTRODUCTION

Spectral analysis is frequently used to study beat-to-beat fluctuations in signals of bioelectric origin. In many bioelectric signals the power in different spectral regions can be linked to various physiological mechanisms. For example, the high-frequency region (HF, 0.15-0.40 Hz) in the heart rate variability (HRV) normally reflects the respiratory related activity in the autonomic control of blood circulation. The-low frequency region (LF, 0.05-0.15 Hz) is linked to the response of the baroreceptor reflex. The fluctuations below 0.05 Hz are related to many factors, such as vasomotion, thermoregulation and other non-stationary control systems [1].

In many clinical studies, power spectrum analysis of HRV data is based on the fast Fourier transform (FFT) or autoregressive (AR) algorithms. These methods relies on the assumption that the signal is stationary, at least during short-term segments. In a recent study, we proposed how the adapted wavelet transforms can be used to analyze and quantify the components in the HRV spectrum [2]. These methods include wavelet packets (WP) and cosine packets (CP) and were chosen because the signal can be analyzed and quantified at different scales, i.e., long time windows can be used to analyze the low frequency components and short windows for the high frequency components in the signal.

The purpose of this study is to apply the WP and CP methods to HRV signals obtained from healthy subjects during provocative maneuvers and compare the results with the classical methods (FFT and AR).

2. METHOD

HRV data was obtained from 20 healthy normal subjects (age 20-40 years, 10 male and 10 female). A single-lead ECG was recorded at 500 Hz and stored in a computer. The recordings started with the subject lying down and having normal spontaneous breathing for six min. This was followed by four sequences each lasting one min: controlled breathing at six breaths/min, rest, 12 breaths/min and rest. The recordings continued for approximately four min after passive tilt to a 70-degree upright position. The R-R intervals were transformed to a heart rate time series by cubic spline interpolation and resampling at a frequency of 2.5 Hz.

The decomposition of the signal with the discrete WP transform, is based on a partition in the frequency plane using a quadrature mirror filter bank. The filter bank consists of pairs of highpass and lowpass filters organized in a tree-structure, where the signal at each scale is decomposed into its detail (highpass component) and approximation (lowpass) signals and downsampled [3]. At each scale the frequency axis is recursively divided in halves. The transform coefficients are the outputs from the filters.

The basis functions for the CP transform, are cosines multiplied by smooth cutoff functions [3]. This is in contrast to the Fourier analysis, where the basis functions are of infinite duration. The CP algorithm is based on a segmentation in the time plane, where the segments of the signal are recursively divided into halves.

Both transform methods results in an orthogonal decomposition of the time series [3,4]. The power in the LF (0.02-0.15 Hz) and HF (0.15-0.40 Hz) bands, therefore was calculated as the log-transform of the sum of the magnitude square of the transform coefficients within each frequency band [2]. In this study we used an uniform partition of the frequency and time axes.

All HRV recordings were detrended to reduce the non-stationary component in the signal using an algorithm based on the discrete wavelet transform as described earlier [2]. This essentially resulted in high-pass filtering with a sharp cut-off frequency at f=0.0195 Hz.

Because many clinical studies of HRV are based on the estimated band power, with less focus on the location of spectral peaks within the frequency bands,